A Note on Different Source Models for Dipole Antennas in GHz Frequency Range

D. Poljak, V. Doric
University od Split /FESB, Split, Croatia
dpoljak@fesb.hr, vdoric@fesb.hr

ICEAA - IEEE APWC 25
International Conference on Electromagnetics in Advanced Applications
IEEE-APS Topical Conference on Antennas and Propagation in Wireless Communications
SEPTEMBER 8-12, 2025
PALERMO, ITALY

This work was supported by the Croatian Science Foundation under the project number **HRZZ- IPS-2024-02-7779.**

ICEAA INTERNATIONAL CONFERENCE ON ELECTROMAGNETICS IN ADVANCED APPLICATIONS
IEEE APWC IEEE-APS TOPICAL CONFERENCE ON ANTENNAS AND PROPAGATION IN WIRELESS COMMUNICATIONS
SEPTEMBER 8-12, 2025
PALERMO, ITALY

ICEAA INTERNATIONAL CONFERENCE ON ELECTROMAGNETICS IN ADVANCED APPLICATIONS
IEEE APWC IEEE-APS TOPICAL CONFERENCE ON ANTENNAS AND PROPAGATION IN WIRELESS COMMUNICATIONS
SEPTEMBER 8-12, 2025
PALERMO, ITALY

CONTENTS

- **INTRODUCTION**
- **FORMULATION**
  - ***Rigorous Integro-Differential Equation Approach***
  - ***Radiated Field Formulas***
- **NUMERICAL SOLUTION**
  - ***Current Distribution***
  - ***Radiated Field***
- **ILLUSTRATIVE EXAMPLES**
  - ***Dipole in free space***
  - ***Vertical dipoles above a lossy half-space***
- **CONCLUDING REMARKS**

ICEAA INTERNATIONAL CONFERENCE ON ELECTROMAGNETICS IN ADVANCED APPLICATIONS
IEEE APWC IEEE-APS TOPICAL CONFERENCE ON ANTENNAS AND PROPAGATION IN WIRELESS COMMUNICATIONS
SEPTEMBER 8-12, 2025
PALERMO, ITALY

INTRODUCTION

- Assesment of human exposure to HF fields requires 3 steps;

- determination of external fields radiated by various EMI sources,
- evaluation of internal fields,
- related local temperature increase.

- Simple geometry of dipole antenna is shown to be useful in the studies of human exposure to *mm* waves corresponding to 5G mobile systems carried out by various WGs under Sc6 of IEEE ICES (International committee on Electromagnetic Safety).
- Analysis of dipole antennas either in free space, or in the presence of a lossy half-space (homogeneous or multilayered), requires a choice of a voltage source at the feed-gap.
- The most commonly used, and also the simplest voltage source model is the delta-gap (DG) source, while the magnetic frill (MF) and magnetic current loop (MCL) source have been used in an appreciably less extent.

INTRODUCTION

Basic restrictions in HF range

6 GHz

f (GHz)

SPECIFIC ENERGY ABSORPTION RATE

ICNIRP 2020
IEEE 2019

ABSORBED POWER DENSITY

$$SAR_V = \frac{\int_V \sigma |\vec{E}|^2 \mathbf{dV}}{2 \int_V \rho \mathbf{dV}} \left[\frac{W}{kg}\right]$$

$$APD = \frac{\iint_A Re[\vec{E} \times \vec{H}^*] d\vec{S}}{2A} \left[\frac{W}{m^2}\right]$$

$A = 1\,cm^2$ or $4\,cm^2$

V – volume of a given mass → whole body, 10g

$\vec{E}(\vec{r})$ … electric field peak value
σ … tissue electric conductivity
ρ … tissue mass density

alternative…

TRANSMITTED POWER DENSITY

$$TPD = \frac{1}{2} \int \sigma(\vec{r}) |\vec{E}(\vec{r})|^2 dz \left[\frac{W}{m^2}\right]$$

ICNIRP public consultation document

A. Šušnjara Nejašmić & D. Poljak, "Impact of Different Voltage Source Models on Radiated Field and IPD within the BEM Formalism", EMC+SIPI, Phoenix, Arizona, USA, Aug 5-9, 2024

INTRODUCTION

→ IEEE 2019 & ICNIRP 2020
- **APD** is basic restriction
- **IPD** is reference level

- **Assessment** of APD above 6 GHz → **tedious task**
- **Different numerical tools** and **averaging schemes** for APD computation.
- **Reliability** of numerical results **with regard to** different **codes**! → IEEE ICES TC95/SC6 WG
- TG6: *EPD/APD Average Methods Li/Kodera/Poljak*
- **Reliability** of results **with regard to** set of **input parameters**! → STOCHASTIC-DETERMINISTIC DOSIMETRY (ongoing and future activities)

Basic restriction: Absorbed power density & Reference level: Incident Power Density above 6 GHz

Some IEEE ICES TC95/SC6 WGs recent publications:

- Li, K., Kodera, S., **Poljak, D.**, Diao, Y., Sasaki, K., Zhang, S. Yao, M., Kapetanovic, A., Li, C., Wu, Tongning et al. **Spatially Averaged Epithelial/Absorbed Power Density for Nonplanar Skin Models Exposed to Antenna at 10–90 GHz,** IEEE access, 12 (2024).
- Li K., Kodera, S., **Poljak, D.** Diao, Y., Sasaki, K., Šušnjara, A., Prokop, A., Taguchi, K. Xi, J., Zhang, S., et al. **Calculated Epithelial/Absorbed Power Density for Exposure from Antennas at 10–90 GHz: Intercomparison Study Using a Planar Skin Model,** *IEEE access* (2023).
- Li, K. Diao, Y., Sasaki, K., Prokop, A., **Poljak, D.**, Dorić, V., Xi, J., Kodera, S., Hirata, A., El Hajj, W., **Intercomparison of Calculated Incident Power Density and Temperature Rise for Exposure From Different Antennas at 10–90 GHz**, IEEE access, 9 (2021).

- Analysis of transmitting wire antennas above lossy media using numerical methods requires **modeling of a voltage source**, provided the feed-gap area is electrically small.
- The choice of a particular feed gap has been shown to appreciably influence the near field behaviour, (e.g., the antenna admittance calculation).
- No appreciable impact on the far field has been observed.
- The most commonly used approaches to source modeling problems:
  - delta-gap (DG) source and
  - magnetic frill (MF) source.

Different voltage source models

Some our recent publications:

- A. Šušnjara and **D. Poljak**, "**Uncertainty Quantification of Epithelial/Absorbed Power Density** in 1-layered Planar Skin Model with Uncertain Tissue Electric Properties, 2023 XXXVth General Assembly and Scientific Symposium of the International Union of Radio Science (URSI GASS) / Sapporo: Institute of Electrical and Electronics Engineers (IEEE), 2023. str. 1-4.
- A. Šušnjara and **D. Poljak**, "Impact of Different Voltage source Models on **Antenna Current and Input Impedance** Within the Boundary Element Method Formalism," 2023 24th International Conference on Applied Electromagnetics and Communications (ICECOM), Dubrovnik, Croatia, 2023, pp. 1-5.
- A. Šušnjara Nejašmić and **D. Poljak**, " Impact of Different Voltage Source Models on **Absorbed Power Density** Within the Boundary Element Method Formalism," 9th International Conference on Smart and Sustainable Technologies (SpliTech), Bol, Croatia, 2024, pp. 1-6.

INTRODUCTION

ICEAA INTERNATIONAL CONFERENCE ON ELECTROMAGNETICS IN ADVANCED APPLICATIONS
IEEE APWC IEEE-APS TOPICAL CONFERENCE ON ANTENNAS AND PROPAGATION IN WIRELESS COMMUNICATIONS
SEPTEMBER 8-12, 2025
PALERMO, ITALY

- This paper addresses the influence of the use of DG, MF and MCL models to current distribution, radiated field and input admittance for dipole antenna in free space and in the presence of a lossy half-space, when used in GHz frequency range.
- The antenna current is governed by the Pocklington IDE while the radiated field is obtained by solving field integrals over squared current.
- Pocklington equation is handled via GB-IBEM providing the evaluation of radiated field and input impedance.

FORMULATION

ICEAA INTERNATIONAL CONFERENCE ON ELECTROMAGNETICS IN ADVANCED APPLICATIONS
IEEE APWC IEEE-APS TOPICAL CONFERENCE ON ANTENNAS AND PROPAGATION IN WIRELESS COMMUNICATIONS
SEPTEMBER 8-12, 2025
PALERMO, ITALY

- The geometry of the problem is a dipole antenna of length L and radius a, insulated in free space or vertically located above a dissipative half-space, and driven by corresponding voltage source model.
- Figure 1 shows 3 different source models; (a) Delta gap (DG); (b) Magnetic frill (MF); (c) Magntetic current loop (MCL)
- The wire dimensions satisfy the conditions required by the thin wire approximation (TWA).

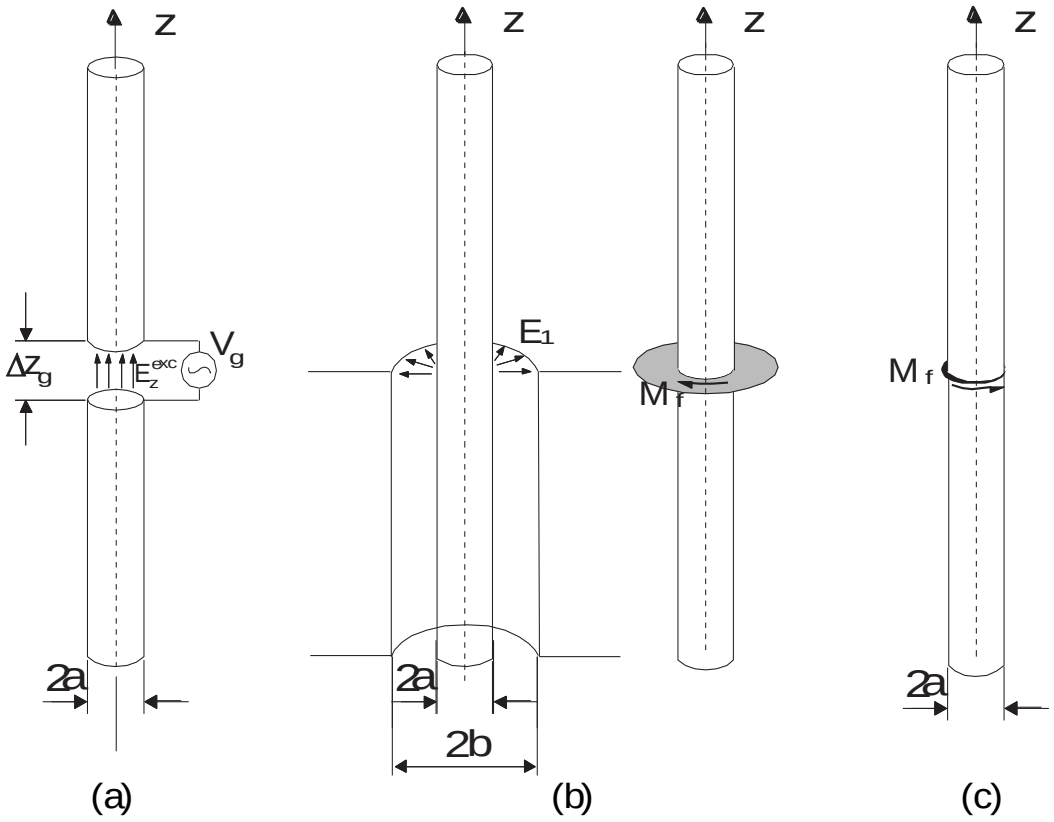

Various types of antenna excitation: (a) Delta gap; (b) Magnetic frill; (c) Magntetic current loop

ICEAA INTERNATIONAL CONFERENCE ON ELECTROMAGNETICS IN ADVANCED APPLICATIONS
IEEE APWC IEEE-APS TOPICAL CONFERENCE ON ANTENNAS AND PROPAGATION IN WIRELESS COMMUNICATIONS
SEPTEMBER 8-12, 2025
PALERMO, ITALY

FORMULATION

Rigorous Integro-Differential Equation Approach

- Modeling of wire antennas in a presnce of a lossy medium is based on the set of coupled Pocklington IDEs .
- Provided the current distribution along a given wire configuration is determined it is possible to calculate the related radiated field by using corresponding integral expressions.
- A general geometry of an arbitrary wire and its image, respectively is shown in Fig 2.

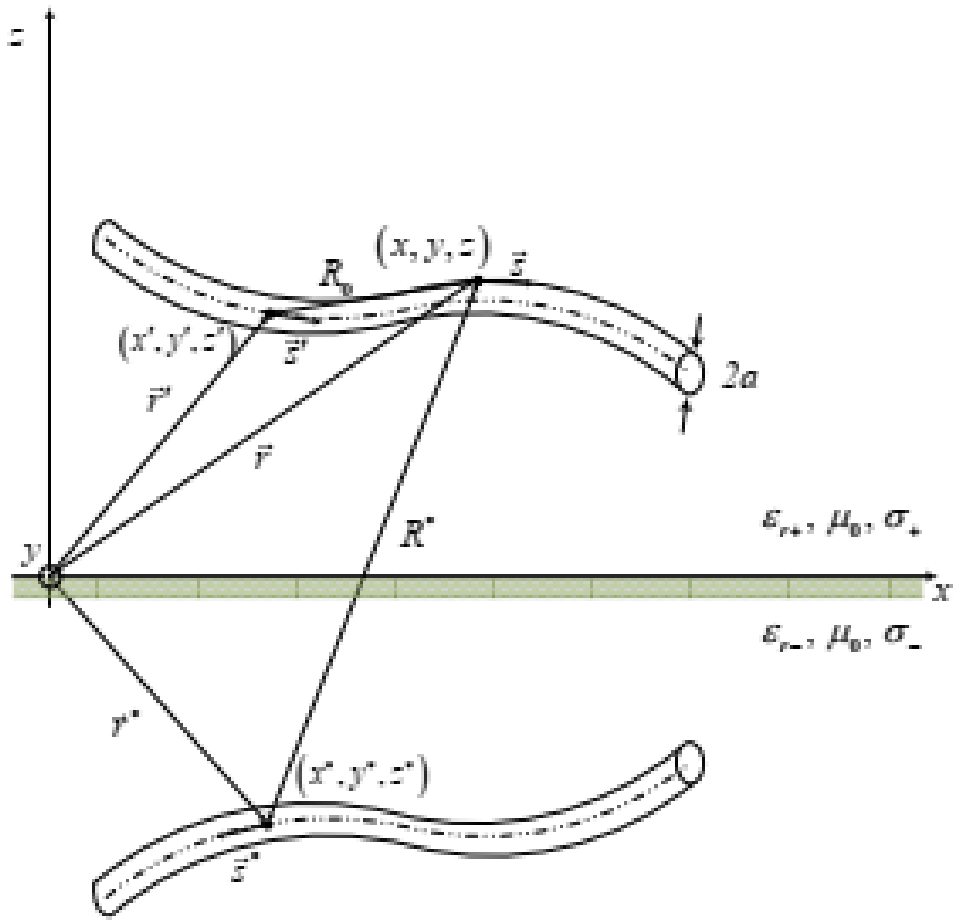

Figure 2. Curved wire configuration and its image

ICEAA INTERNATIONAL CONFERENCE ON ELECTROMAGNETICS IN ADVANCED APPLICATIONS
IEEE APWC IEEE-APS TOPICAL CONFERENCE ON ANTENNAS AND PROPAGATION IN WIRELESS COMMUNICATIONS
SEPTEMBER 8-12, 2025
PALERMO, ITALY

FORMULATION

Rigorous Integro-Differential Equation Approach

- The corresponding integro-differential equation set is given by

$$E_{sm}^{exc}(s) = \frac{j}{4\pi\omega\varepsilon_0}\sum_{n=1}^{N_w}\int_0^{L_n}\left\{\left[k^2\,\vec{e}_{s_m}\vec{e}_{s_n'} - \frac{\partial^2}{\partial s_m \partial s_n'}\right]g_{0n}(s_m, s_n') + R^{tot}\left[k^2\,\vec{e}_{s_m}\vec{e}_{s_n^*} - \frac{\partial^2}{\partial s_m \partial s_n^*}\right]g_{in}(s_m, s_n^*)\right\} I(s_n')ds'$$

$$g_{0mn}(s_m, s_n') = \frac{e^{-jk\ R_{1mn}}}{R_{1mn}}\ ,\ g_{imn}(s_m, s_n') = \frac{e^{-jk\ R_{2mn}}}{R_{2mn}} \qquad \varepsilon_{effm,n} = \varepsilon_{rm,n} - j\frac{\sigma_{m,n}}{\omega}$$

while the total reflection coefficient to account for the reflection between air and layered lower medium, arising from the extended use of the modified image theory is

$$R^{tot} = \frac{R_{12}+R_{23}e^{-2\gamma_2 d}}{1+R_{12}R_{23}e^{-2\gamma_2 d}} \qquad R_{mn} = \frac{\varepsilon_{eff,m}-\varepsilon_{eff,n}}{\varepsilon_{eff,m}+\varepsilon_{eff,n}}$$

FORMULATION

Rigorous Integro-Differential Equation Approach

Voltage source models

Delta gap (DG) ⟷ Magnetic frill (MF)

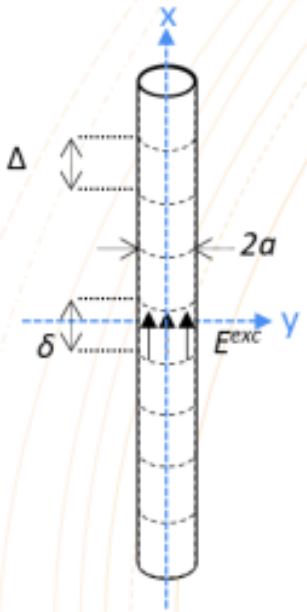

$\Delta = L/N$, N…odd number

a & b… radius of inner & outer MF annular aperture

a… antenna radius

E^i… incident field

E^{exc}… excitation field

M_Φ… magnetic current generated

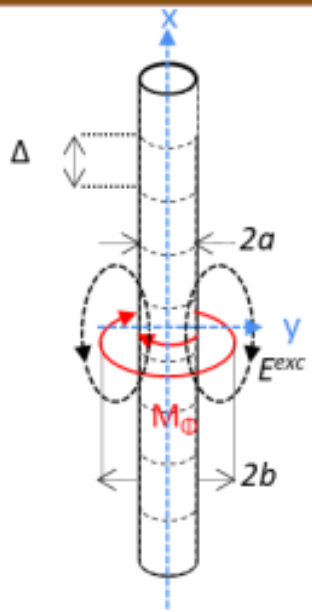

$$E^{exc}(x) = E^{DG}(x) = \begin{cases} \frac{U}{\delta}, |x| \le \delta \\ 0, otherwise \end{cases}$$

$\delta = \Delta$

$$E^{exc}(x) = E^{MF}(x) = \frac{V}{2\,ln(b/a)}\left[\frac{e^{(-jkR_a)}}{R_a} - \frac{e^{(-jkR_b)}}{R_b}\right]$$

$$Z_C = \frac{1}{2\pi}\sqrt{\frac{\mu_0}{\varepsilon_0}}ln\left(\frac{b}{a}\right) \qquad R_a = \sqrt{x^2 + a^2}, \qquad R_b = \sqrt{x^2 + b^2}$$

When $b=a$ and $\delta \to 0$: $E^{MF}(x) = \frac{a^2\,V}{2}\frac{1 + jkR_a}{R_a^3}e^{(-jkR_a)}$

FORMULATION

Rigorous Integro-Differential Equation Approach

ICEAA INTERNATIONAL CONFERENCE ON ELECTROMAGNETICS IN ADVANCED APPLICATIONS
IEEE APWC IEEE-APS TOPICAL CONFERENCE ON ANTENNAS AND PROPAGATION IN WIRELESS COMMUNICATIONS
SEPTEMBER 8-12, 2025
PALERMO, ITALY

- The delta gap source model assumes the excitation electric field to exist only in the gap between the antenna input terminals and is zero outside.
- The impressed field in the gap between terminals is:

$$E_z^{exc} = \frac{V_g}{\Delta z}$$

- In MF source model, the gap is replaced with a circularly directed magnetic current density that exists over the annular aperture with inner radius *a* (usually radius of the wire) and an outer radius *b*. This magnetic frill generates field on the axis of the wire which excites the antenna:

$$E_z^{exc} = \frac{1}{2}\frac{V_g}{\ln\left(\frac{b}{a}\right)}\left[\frac{e^{-jk\sqrt{a^2+(z-z')^2}}}{\sqrt{a^2+(z-z')^2}} - \frac{e^{-jk\sqrt{b^2+(z-z')^2}}}{\sqrt{b^2+(z-z')^2}}\right]$$

- As an antenna is usually fed by a transmission line, radius *b* is found using the expression for characteristic impedance of the transmission line.
- Therefore, radius *b* is not always known.
- The simple magnetic current loop (MCL), with unit magnetic current density, generates axial electric field that feeds the antenna:

$$E_z(0,z) = \frac{a^2}{2}\left[jk + \frac{1}{\sqrt{a^2+(z-z')^2}}\right]\frac{e^{-jk\sqrt{a^2+(z-z')^2}}}{a^2+(z-z')^2}$$

- This type of source can be derived from the both delta gap and magnetic frill.

FORMULATION

Rigorous Integro-Differential Equation Approach

ICEAA INTERNATIONAL CONFERENCE ON ELECTROMAGNETICS IN ADVANCED APPLICATIONS
IEEE APWC IEEE-APS TOPICAL CONFERENCE ON ANTENNAS AND PROPAGATION IN WIRELESS COMMUNICATIONS
SEPTEMBER 8-12, 2025
PALERMO, ITALY

- In the delta gap source, the electric field can be replaced with the narrow strip of equivalent magnetic current density

$$\overrightarrow{M}_g = -\vec{n}\times\vec{E}_z^{exc} = -\vec{e}_\rho\times\vec{e}_z\frac{V_g}{\Delta z} = \vec{e}_\phi\frac{V_g}{\Delta z};\qquad -\frac{\Delta z}{2}\le z'\le\frac{\Delta z}{2}$$

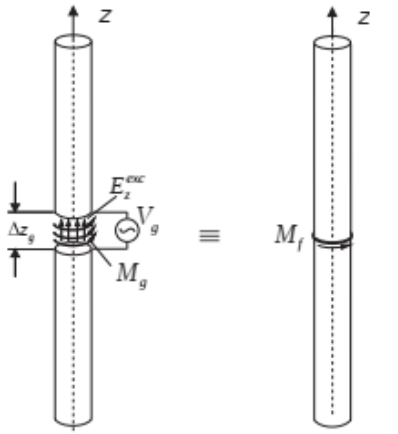

Delta gap source and simple magnetic current loop

- In the particular limiting case when $\Delta z \to 0$, and unit voltage, the axial electric field of narrow magnetic strip acquires the MCL form.

- Another way to derive the MCL source model is to start from MF source.
- Namely, if *b* approaches *a* in MF yields:

$$E_z(0,z) = \lim_{b\to a}\left\{\frac{1}{2}\frac{V_0}{\ln\left(\frac{b}{a}\right)}\left[\frac{e^{-jk\sqrt{b^2+(z-z')^2}}}{\sqrt{a^2+(z-z')^2}} - \frac{e^{-jk\sqrt{b^2+(z-z')^2}}}{\sqrt{b^2+(z-z')^2}}\right]\right\}$$

one obtains the expression for axial electric field of MCL source.

FORMULATION

Radiated Fields Formulas

- The total electric and magnetic fields irradiated by a configuration of multiple wires of arbitrary shape are given by

$$\vec{E} = \sum_{n=1}^{N_w} \left[\vec{E}_{0n} + R^{tot} \cdot \vec{E}_{in} \right]$$

$$\vec{H} = \sum_{n=1}^{N_w} \left[\vec{H}_{Sn} + R^{tot} \cdot \vec{H}_{In} \right]$$

$$\vec{E}_{0n} = \frac{1}{j4\pi\omega\varepsilon_0} \left[k_1^2 \int_0^{L_n} \vec{e}_{s_n} I(s_n') g_{0n}(\vec{r},\vec{r}') ds_n' + \int_0^{L} \frac{\partial I(s_n')}{\partial s_n'} \nabla g_{0n}(\vec{r},\vec{r}') ds_n' \right] \qquad \vec{H}_{Sn} = -\frac{1}{4\pi} \int_0^{L_n} I(s_n') \vec{e}_{s_n} \times \nabla g_{0n}(\vec{r},\vec{r}') ds'$$

$$\vec{E}_{in} = \frac{1}{j4\pi\omega\varepsilon_0} \left[k_1^2 \int_0^{L_n} \vec{e}_{s_n *} I(s'_n) g_{in}(\vec{r},\vec{r}^*) dw' - \int_0^{L_n} \frac{\partial I(s^*)}{\partial s_n^*} \nabla g_{in}(\vec{r},\vec{r}^*) ds' \right] \qquad \vec{H}_{In} = -\frac{1}{4\pi} \int_0^{L_n} I(s_n') \vec{e}_{s^*} \times \nabla g_{in}(\vec{r},\vec{r}^*) ds'$$

NUMERICAL SOLUTION

ICEAA INTERNATIONAL CONFERENCE ON ELECTROMAGNETICS IN ADVANCED APPLICATIONS
IEEE APWC IEEE-APS TOPICAL CONFERENCE ON ANTENNAS AND PROPAGATION IN WIRELESS COMMUNICATIONS
SEPTEMBER 8-12, 2025
PALERMO, ITALY

Current distribution

- The Set of Pocklington integro-differential equations is solved via the Galerkin-Bubnov scheme of the Indirect Boundary Element Method (GB-IBEM).

$$\sum_{n=1}^{M}\sum_{i=1}^{N_n}[Z]_{ji}^{e}\{I\}_{i}^{e}=\{V\}_{j}^{e}$$

$$[Z]_{ij}^{e}=-\int_{-1}^{1}\int_{-1}^{1}\{D\}_j\{D'\}_i^T g_{0nm}(s_n,s_m')\frac{ds_m'}{d\xi'}d\xi'\frac{ds_n}{d\xi}d\xi+k_1^2\vec{e}_{s_n}\vec{e}_{s_m}\int_{-1}^{1}\int_{-1}^{1}\{f\}_j\{f'\}_i^T g_{0nm}(s_n,s_m')\frac{ds_m'}{d\xi'}d\xi'\frac{ds_n}{d\xi}d\xi-$$

$$-R_{TM}\int_{-1}^{1}\int_{-1}^{1}\{D\}_j\{D'\}_i^T g_{inm}(s_n,s_m^*)\frac{ds_m'}{d\xi'}d\xi'\frac{ds_n}{d\xi}d\xi+R^{tot}\cdot k_1^2\vec{e}_{s_n}\vec{e}_{s_m}^*\int_{-1}^{1}\int_{-1}^{1}\{f\}_j\{f'\}_i^T g_{inm}(s_n,s_m^*)\frac{ds_m'}{d\xi'}d\xi'\frac{ds_n}{d\xi}d\xi$$

$$\{V\}_j^n=-j4\pi\omega\varepsilon_0\int_{-1}^{1}E_{s_n}^{exc}(s_n)f_{jn}(s_n)\frac{ds_n}{d\xi}d\xi_n$$

NUMERICAL SOLUTION

ICEAA INTERNATIONAL CONFERENCE ON ELECTROMAGNETICS IN ADVANCED APPLICATIONS
IEEE APWC IEEE-APS TOPICAL CONFERENCE ON ANTENNAS AND PROPAGATION IN WIRELESS COMMUNICATIONS
SEPTEMBER 8-12, 2025
PALERMO, ITALY

Radiated Fields

- Once the current distribution is obtained, the radiated electric and magnetic field can be obtained applying the similar BEM formalism:

$$\vec{E} = \sum_{k=1}^{N}\left[\vec{E}^{e}_{Sk} + R^{tot}\cdot\vec{E}^{e}_{Ik}\right]$$

$$\vec{E}^{e}_{Sk} = \frac{1}{j4\pi\omega\varepsilon_0}\sum_{i=1}^{n}\left[k^2\int_{-1}^{1}\vec{e}_{ks}I^{e}_{ik}f_i(\xi)g_{0k}(\vec{r},\vec{r}')\frac{ds_k'}{d\xi}d\xi + \int_{-1}^{1}I^{e}_{ik}\frac{\partial f_i(\xi)}{\partial\xi}\nabla g_{0k}(\vec{r},\vec{r}')\frac{ds_k'}{d\xi}d\xi\right]$$

$$\vec{E}^{e}_{I} = \frac{1}{j4\pi\omega\varepsilon_0}\sum_{i=1}^{n}\left[k^2\int_{-1}^{1}\vec{e}_{ks*}I^{e}_{ik}f_i(\xi)g_{ik}(\vec{r},\vec{r}^{*})\frac{ds_k'}{d\xi}d\xi - \int_{-1}^{1}I^{e}_{ik}\frac{\partial f_i(\xi)}{\partial\xi'}\nabla g_{ik}(\vec{r},\vec{r}^{*})\frac{ds_k'}{d\xi}d\xi\right]$$

$$\vec{H} = \sum_{k=1}^{N}\left[\vec{H}^{e}_{Sk} + R^{tot}\cdot\vec{H}^{e}_{Ik}\right]$$

$$\vec{H}^{e}_{Sk} = -\frac{1}{4\pi}\sum_{i=1}^{n}\int_{-1}^{1}I_{ik}f_i(\xi)\vec{e}_{s_k'}\times\nabla g_{0k}(\vec{r},\vec{r}')\frac{ds_k'}{d\xi}d\xi$$

$$\vec{H}^{e}_{Ik} = -\frac{1}{4\pi}\sum_{i=1}^{n}\int_{-1}^{1}I^{e}_{ik}f_i(\xi)\vec{e}_{ks*}\times\nabla g_{ik}(\vec{r},\vec{r}^{*})\frac{ds_k'}{d\xi}d\xi$$

ILLUSTRATIVE EXAMPLES

ICEAA INTERNATIONAL CONFERENCE ON ELECTROMAGNETICS IN ADVANCED APPLICATIONS
IEEE APWC IEEE-APS TOPICAL CONFERENCE ON ANTENNAS AND PROPAGATION IN WIRELESS COMMUNICATIONS
SEPTEMBER 8-12, 2025
PALERMO, ITALY

- Numerical results for the current distribution, radiated field and input impedance for the dipole in free space and vertically located above a lossy half-space, respectively, are obtained.
- Consider dipole antenna L=0.1m long, with a radius of a=0.5mm excited by the voltage source V_T=1V.
- The source is modelled as a DG with constant electric field, MF and MCL, respectively.
- In the MF case ratio b/a = 2.3 corresponds to the typical 50Ω coaxial cable excitation.

ILLUSTRATIVE EXAMPLES

ICEAA INTERNATIONAL CONFERENCE ON ELECTROMAGNETICS IN ADVANCED APPLICATIONS
IEEE APWC IEEE-APS TOPICAL CONFERENCE ON ANTENNAS AND PROPAGATION IN WIRELESS COMMUNICATIONS
SEPTEMBER 8-12, 2025
PALERMO, ITALY

Dipole in free space

- The results for the current distribution along the wire obtained via different excitation approaches at typical 5G operating frequencies are presented in Figs 2 to 6.
- The wire is discretized into 31 segments in all cases.

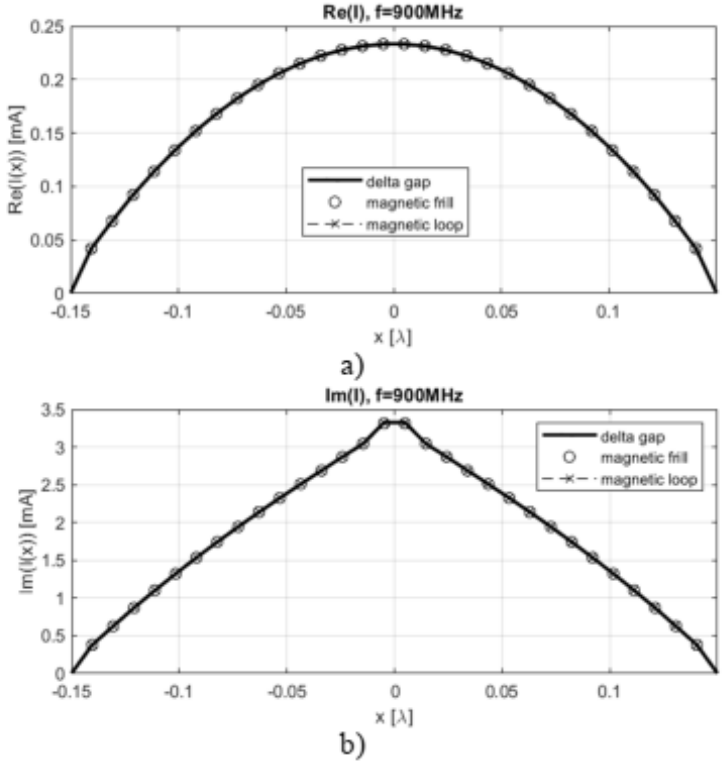

Fig 2. a) Real part and b) imaginary part of the current distribution along the dipole at f=900MHz

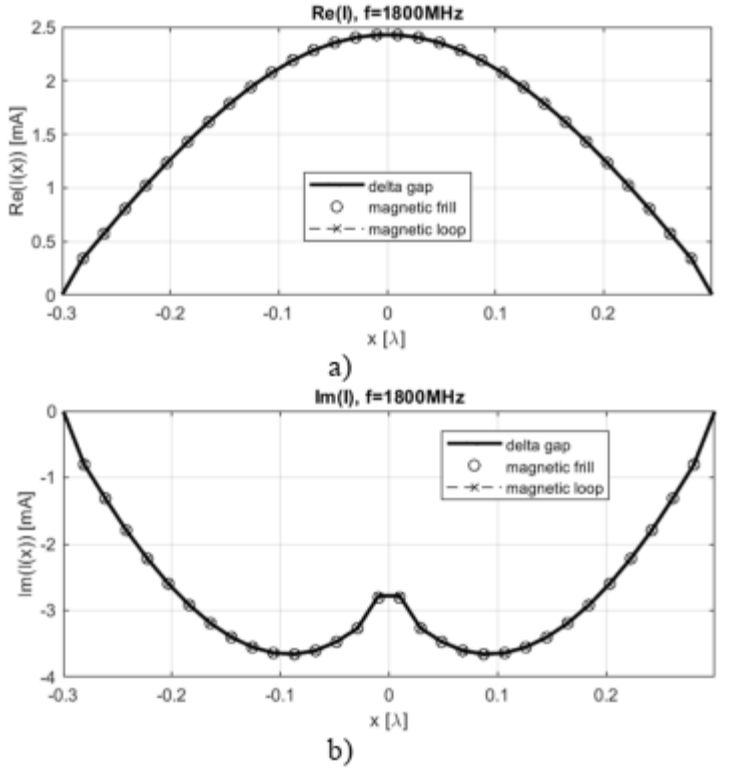

Fig 3. a) Real part and b) imaginary part of the current distribution along the dipole at f=1.8 GHz

ILLUSTRATIVE EXAMPLES

Dipole in free space

ICEAA INTERNATIONAL CONFERENCE ON ELECTROMAGNETICS IN ADVANCED APPLICATIONS
IEEE APWC IEEE-APS TOPICAL CONFERENCE ON ANTENNAS AND PROPAGATION IN WIRELESS COMMUNICATIONS
SEPTEMBER 8-12, 2025
PALERMO, ITALY

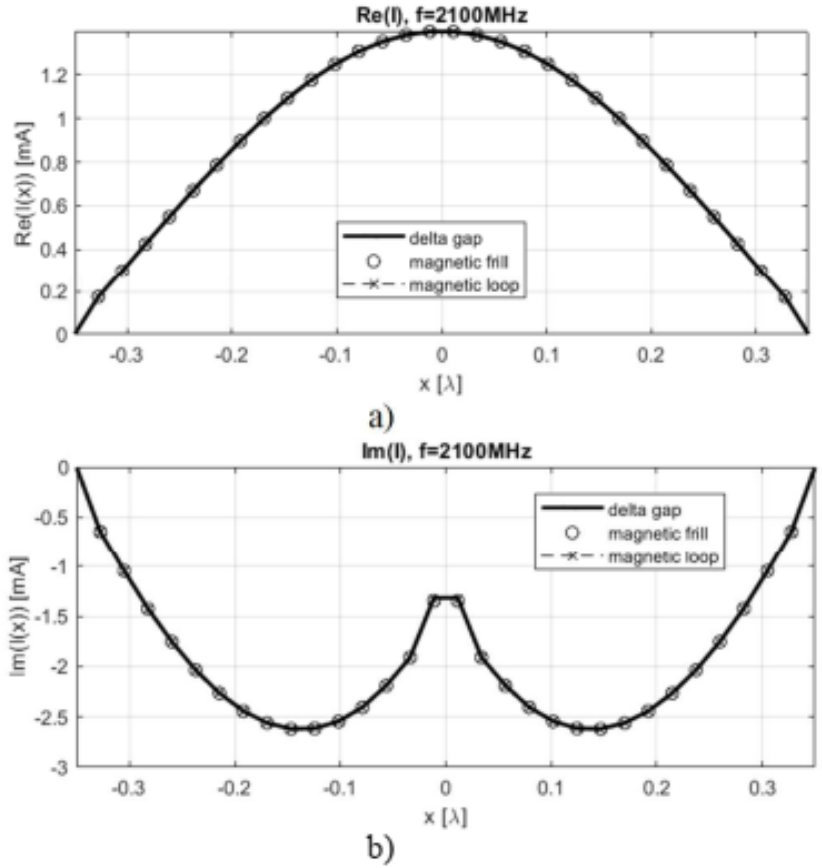

Fig 4. a) Real part and b) imaginary part of the current distribution along the dipole at *f*=2.1GHz

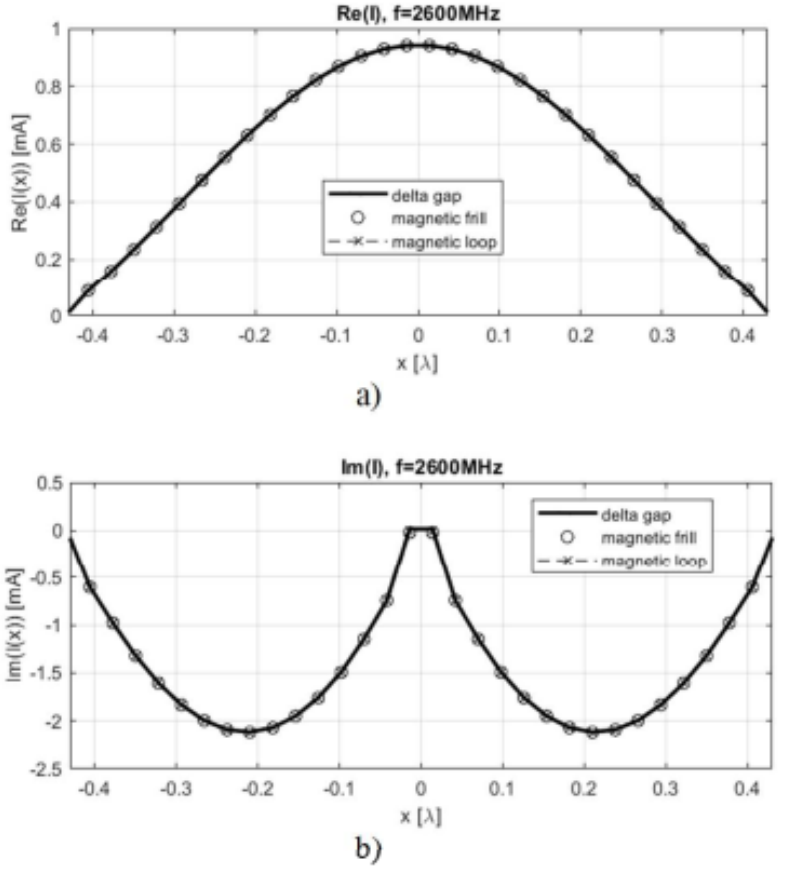

Fig 5. a) Real part and b) imaginary part of the current distribution along the dipole at *f*=2.6GHz

ILLUSTRATIVE EXAMPLES

ICEAA INTERNATIONAL CONFERENCE ON ELECTROMAGNETICS IN ADVANCED APPLICATIONS
IEEE APWC IEEE-APS TOPICAL CONFERENCE ON ANTENNAS AND PROPAGATION IN WIRELESS COMMUNICATIONS
SEPTEMBER 8-12, 2025
PALERMO, ITALY

Dipole in free space

- Excellent agreement between different methods could be observed.
- Fig 7 shows the real and imaginary part of the current at the feed point a part of the spectrum in GHz frequency range. In this case the dipole is discretized into 51 segments.

- There is a satisfactory agreement between the results obtained via different source models.

- Above 7GHz less than 5% discrepancy occurs between DG and MF results for the imaginary part of the driving point current.

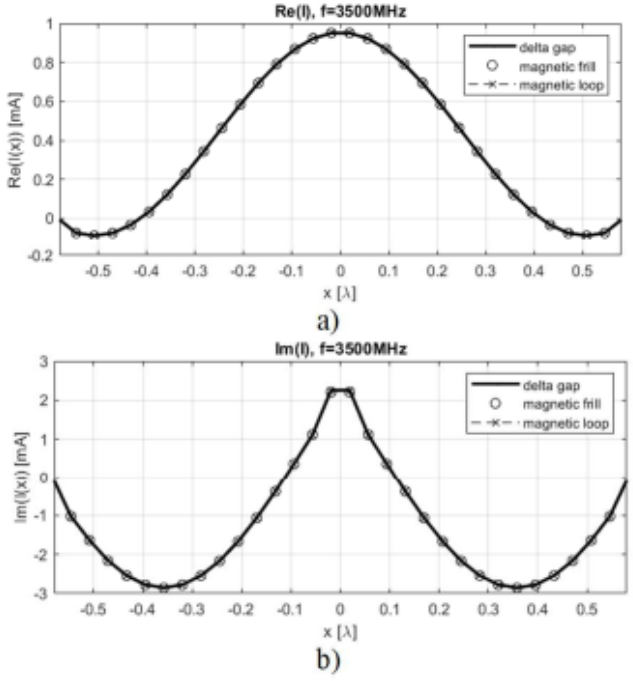

Fig 6. a) Real part and b) imaginary part of the current distribution along the dipole at f=3.5GHz

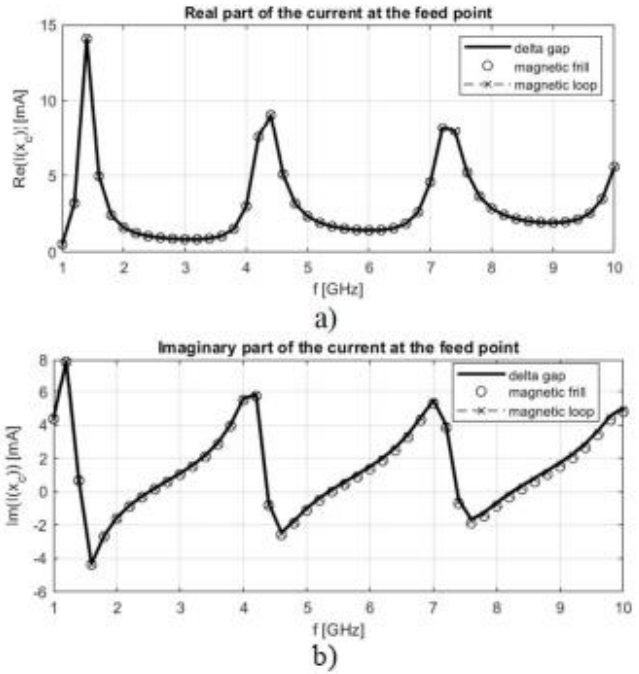

Fig 7. Frequency spectrum of the a) real and b) imaginary part of the current at the feed point

ILLUSTRATIVE EXAMPLES

ICEAA INTERNATIONAL CONFERENCE ON ELECTROMAGNETICS IN ADVANCED APPLICATIONS
IEEE APWC IEEE-APS TOPICAL CONFERENCE ON ANTENNAS AND PROPAGATION IN WIRELESS COMMUNICATIONS
SEPTEMBER 8-12, 2025
PALERMO, ITALY

Dipole in free space

- As the central segment is the most influential parameter considering the feed gap current, number of segments is varied from 11 to 101 at f = 9GHz (Fig. 8).

- The maximum value of the feed gap current (in particular the imaginary part) depends on the segment size and the results arising from different source models vary appreciably.

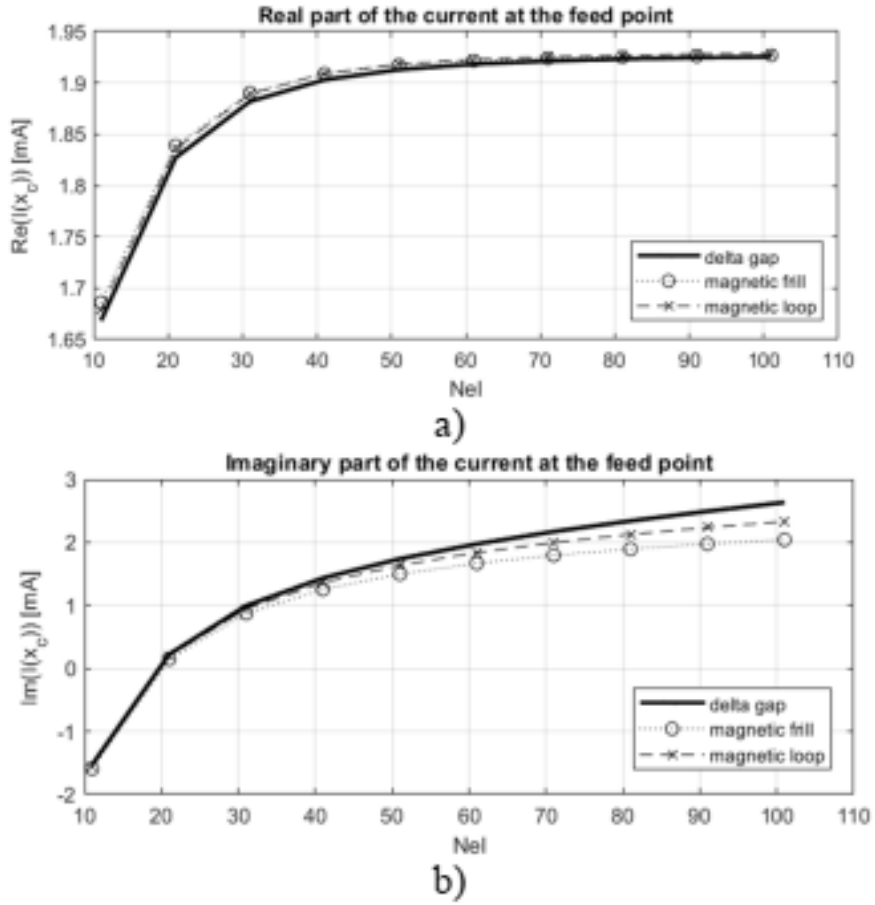

Fig 8. a) Real and b) imaginary part of the current at the feed point vs number of segments along the wire at f = 9GHz

ILLUSTRATIVE EXAMPLES

Dipole in free space

ICEAA INTERNATIONAL CONFERENCE ON ELECTROMAGNETICS IN ADVANCED APPLICATIONS
IEEE APWC IEEE-APS TOPICAL CONFERENCE ON ANTENNAS AND PROPAGATION IN WIRELESS COMMUNICATIONS
SEPTEMBER 8-12, 2025
PALERMO, ITALY

- In Figs 9 and 10 the imaginary part of the current distribution along the dipole is shown for the case of 81 segments.
- The results obtained by different source models show discrepancies in the close vicinity of the feed gap area (see Fig. 10).
- This finding is important as it affects the calculation of the dipole input impedance - one of the crucial important antenna parameters in engineering practice.

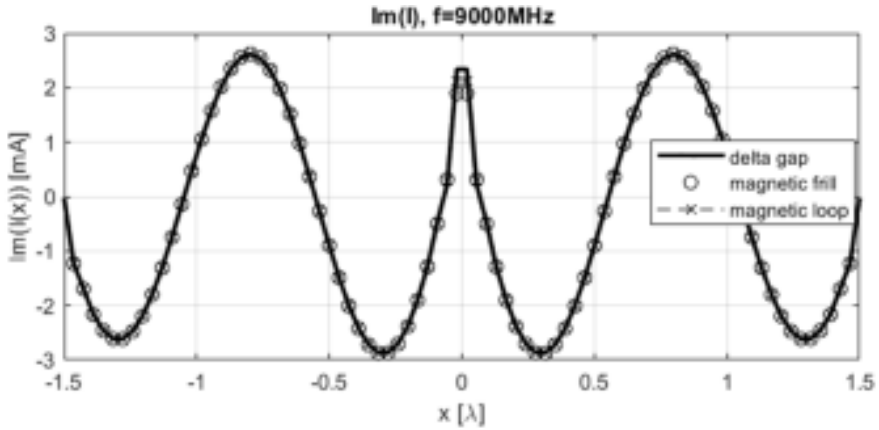

Fig 9. Imaginary part of the current distribution along the dipole for operating frequency $f = 9$GHz

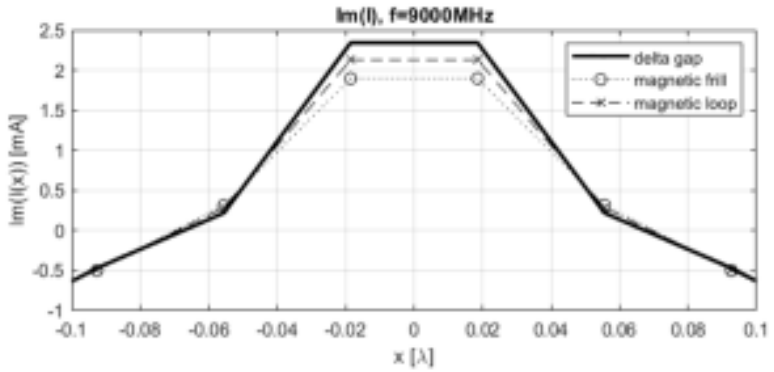

Fig 10. Imaginary part of the current distribution in the vicinity of the feed-gap for operating frequency $f = 9$GHz

ILLUSTRATIVE EXAMPLES

ICEAA INTERNATIONAL CONFERENCE ON ELECTROMAGNETICS IN ADVANCED APPLICATIONS
IEEE APWC IEEE-APS TOPICAL CONFERENCE ON ANTENNAS AND PROPAGATION IN WIRELESS COMMUNICATIONS
SEPTEMBER 8-12, 2025
PALERMO, ITALY

Dipole in free space

- Fig 11 shows the effect of the number of elements and feed gap model on the antenna input impedance. 11.

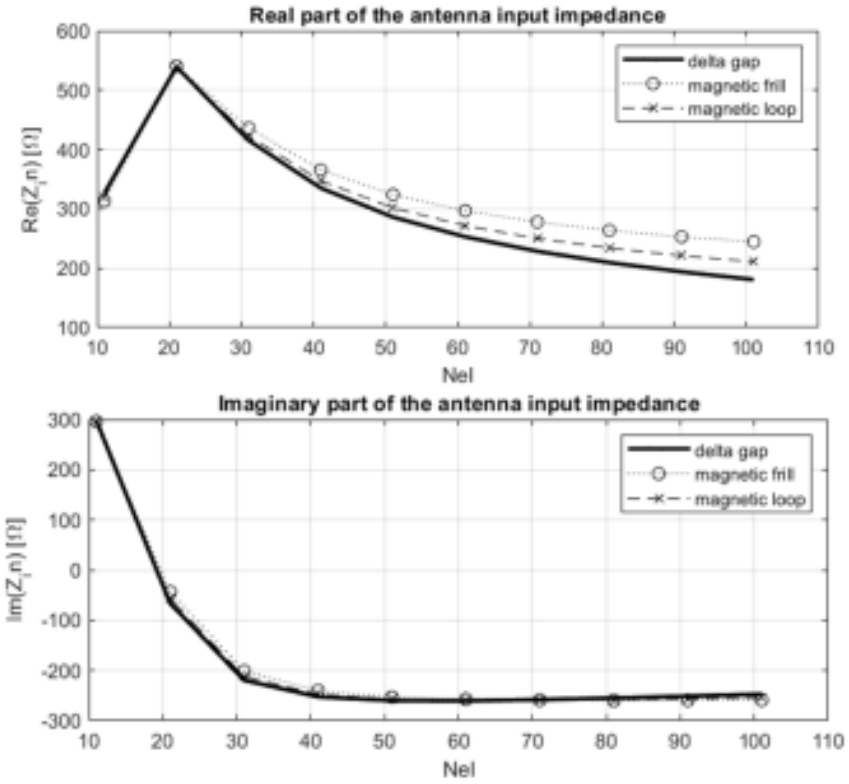

Fig 11. Real and imaginary parts of the input impedance versus number of segments along the wire at f=9GHz

- Tangential component of the radiated electric field is depicted in Fig. 12.

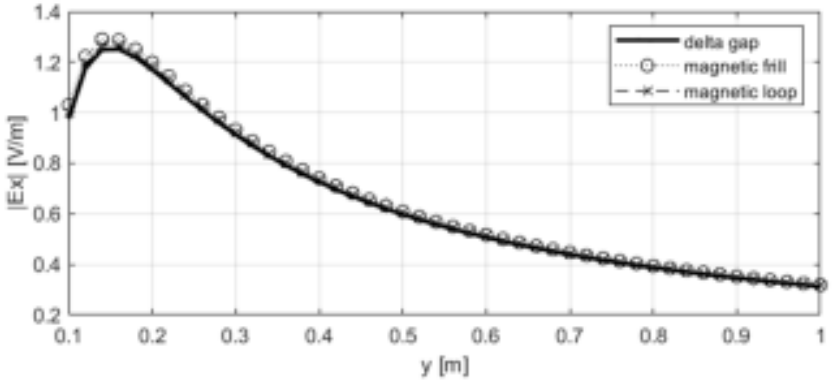

Fig 12. Tangential component of the radiated field in broadside direction for different source models (f=9GHz, N_{el}=81)

- The field values slightly vary only in the feed gap area.
- Otherwise, there is a rather satisfactory agreement between the results obtained by different models.

ILLUSTRATIVE EXAMPLES

ICEAA INTERNATIONAL CONFERENCE ON ELECTROMAGNETICS IN ADVANCED APPLICATIONS
IEEE APWC IEEE-APS TOPICAL CONFERENCE ON ANTENNAS AND PROPAGATION IN WIRELESS COMMUNICATIONS
SEPTEMBER 8-12, 2025
PALERMO, ITALY

Dipole in free space

- Figure 13 shows the broadside field (y=0.15m from the antenna) vs number of wire segments at f=9GHz.
- There is no significant difference between the results, i.e. maximum relative error is 3.33% for the point close to the antenna.
- The electric field results (for input power P_{in}=10mW) are shown in Fig. 14.
- The field values vary more appreciably with the segment size (the maximum difference is 11%, which is more than 3 times higher compared to the case of the fixed impressed voltage).

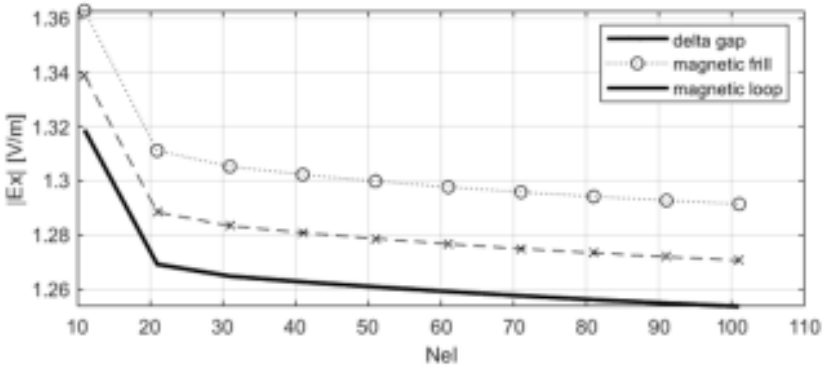

Fig 13. Tangential field component at point (y=0.15m from the antenna, vs number of wire segments at f=9GHz.

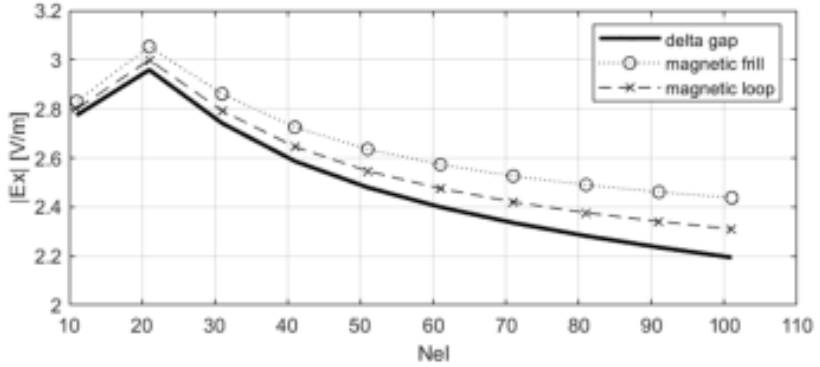

Fig 14. Tangential component of the radiated field at broadside point (y=0.15m from the antenna) versus number of segments along the wire (P_{in} = 10mW, f = 9GHz)

ILLUSTRATIVE EXAMPLES

ICEAA INTERNATIONAL CONFERENCE ON ELECTROMAGNETICS IN ADVANCED APPLICATIONS
IEEE APWC IEEE-APS TOPICAL CONFERENCE ON ANTENNAS AND PROPAGATION IN WIRELESS COMMUNICATIONS
SEPTEMBER 8-12, 2025
PALERMO, ITALY

Vertical dipole above a lossy space

- The same dipole antenna is placed at height h = 6 cm from a lossy ground (σ = 0.001 S/m and ε_r = 10) to the antenna center.

- The current distribution along the wire for different source models for various operating frequencies are shown in Figs 15-18).
- The wire is discretized into 31 segments

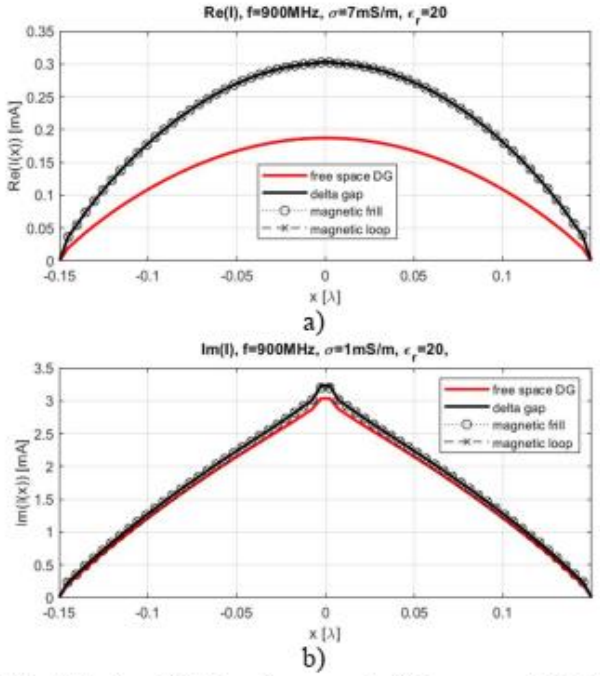

Fig 15. a) Real and b) imaginary part of the current distribution along the dipole at f=900MHz (h=6cm, σ=7mS/m, ε_r=20)

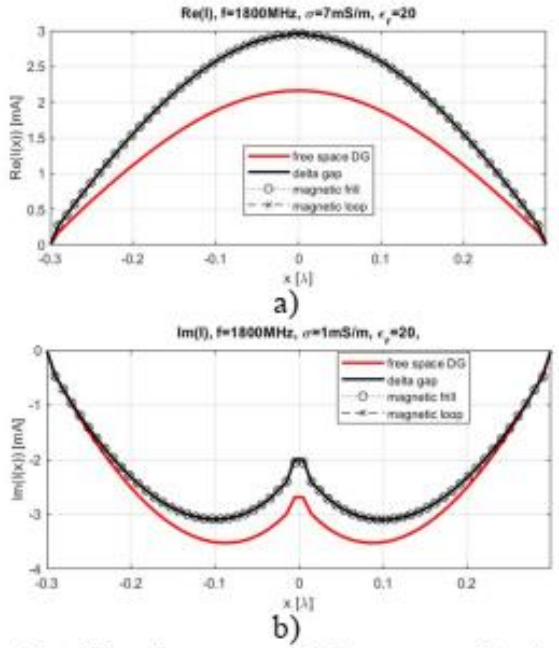

Fig 16. Real and imaginary part of the current distribution along the dipole at f=1800MHz (h=6cm, σ=7mS/m, ε_r=20)

ILLUSTRATIVE EXAMPLES

ICEAA INTERNATIONAL CONFERENCE ON ELECTROMAGNETICS IN ADVANCED APPLICATIONS
IEEE APWC IEEE-APS TOPICAL CONFERENCE ON ANTENNAS AND PROPAGATION IN WIRELESS COMMUNICATIONS
SEPTEMBER 8-12, 2025
PALERMO, ITALY

Vertical dipole above a lossy space

- The lower the frequency, the more pronounced is the influence of the lossy ground to current distribution compared to the free space case (Figs 15-18).
- Such a behaviour is expected as the antenna is closer to the air-ground interface at the lower frequencies.
- Asymmetry in the current distribution, which is expected as one arm of the dipole is closer to the ground, is more noticeable at the higher frequencies is more pronounced for the real part of the current.

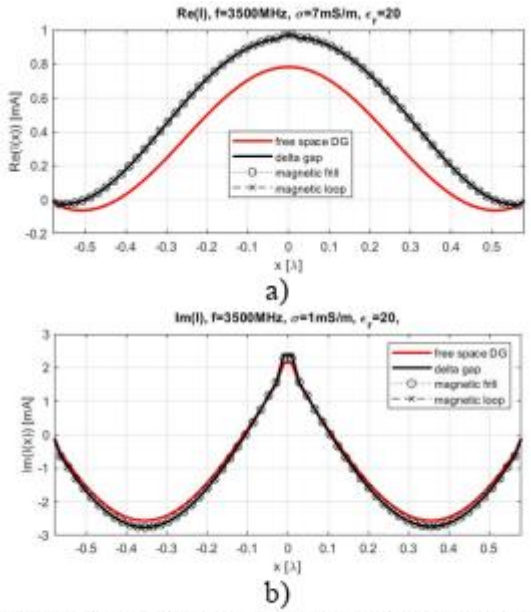

Fig 17. Real and imaginary part of the current distribution along the dipole at f=3.5GHz (h=6cm, σ=7mS/m, ε_r=20)

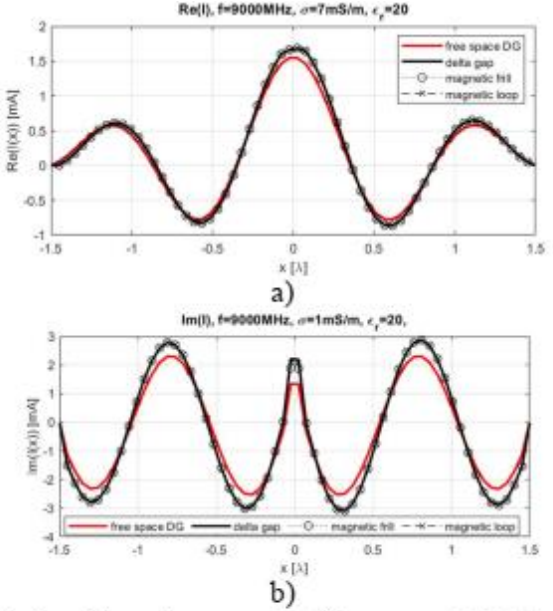

Fig 18. Real and imaginary parts of the current distribution long the dipole at f=9GHz (h=6cm, σ=7mS/m, ε_r=20)

ILLUSTRATIVE EXAMPLES

ICEAA INTERNATIONAL CONFERENCE ON ELECTROMAGNETICS IN ADVANCED APPLICATIONS
IEEE APWC IEEE-APS TOPICAL CONFERENCE ON ANTENNAS AND PROPAGATION IN WIRELESS COMMUNICATIONS
SEPTEMBER 8-12, 2025
PALERMO, ITALY

Vertical dipole above a lossy space

- The real part and imaginary part of the current distribution along the wire above the perfectly conducted (PEC) ground are shown in Fig 19.

- In this case left-right asymmetry is more pronounced compared to the previous examples.

- The current distribution results for the different excitation models (Figs 15-19) show very good agreement for the frequencies of interest except for the imaginary part of the current at the driving point.

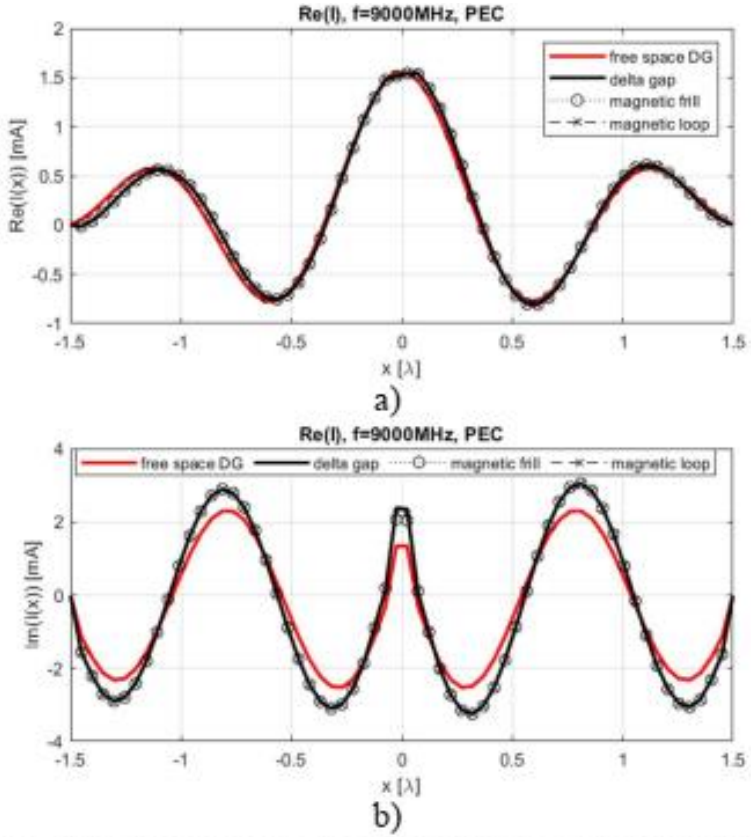

Fig 19. a) Real and b) imaginary part of the current distribution along the dipole above a PEC ground at f=9GHz (h=6cm,)

ILLUSTRATIVE EXAMPLES

Vertical dipole above a lossy space

ICEAA INTERNATIONAL CONFERENCE ON ELECTROMAGNETICS IN ADVANCED APPLICATIONS
IEEE APWC IEEE-APS TOPICAL CONFERENCE ON ANTENNAS AND PROPAGATION IN WIRELESS COMMUNICATIONS
SEPTEMBER 8-12, 2025
PALERMO, ITALY

- Again, as in the case of dipole in free space (Fig. 7), values of the current at the driving point are presented in Fig. 20.
- Note that very similar results are obtained, i.e. small discrepancies between the results are visible for $f > 5$ GHz and only for the imaginary part of the current.
- As it was noted previously, these may lead to different values of input impedance.
- Similar behaviour of the radiated electric field and input impedance is expected.

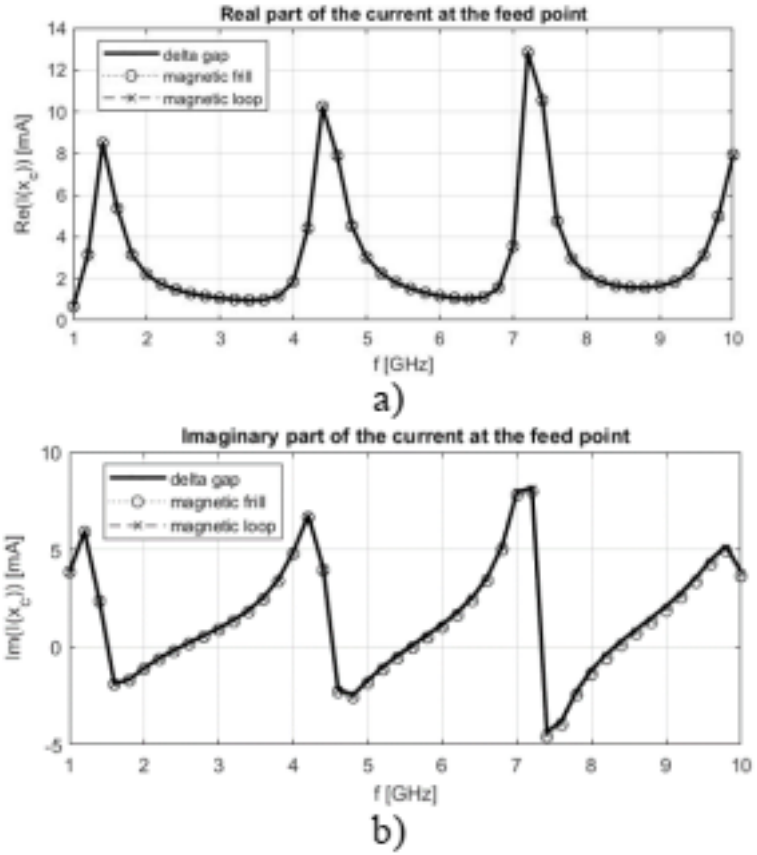

Fig 20. Real and imaginary parts of the current at the feed point vs frequency for dipole at h=6cm above PEC ground.

A Note Regarding Onging Work

ICEAA International Conference on Electromagnetics in Advanced Applications
IEEE APWC IEEE-APS Topical Conference on Antennas and Propagation in Wireless Communications
SEPTEMBER 8-12, 2025
PALERMO, ITALY

Input parameters

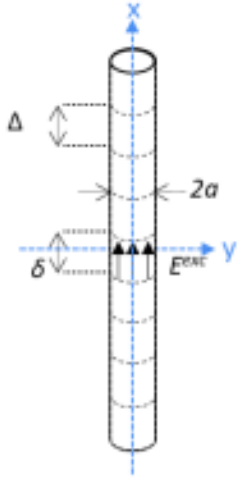

Delta gap (DG)

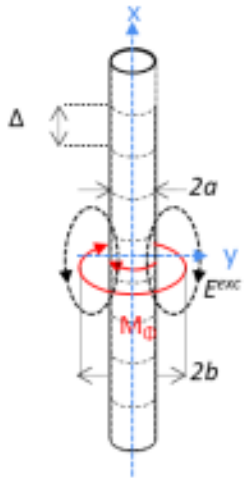

Magnetic frill (MF)

Antenna length: L=0.47*λ

Antenna radius, a:

a_1=L/(N*10)

a_2=0.005*λ

N=31

U=1V

Equivalent voltage values for different antenna radius and MF sources

a_1=L/(N*10)		a_2=λ*0.005	
U_{eq}, b/a=2.3	U_{eq}, b/a=1	U_{eq}, b/a=2.3	U_{eq}, b/a=1
0.9530 V	0.9807 V	0.7031 V	0.8354 V

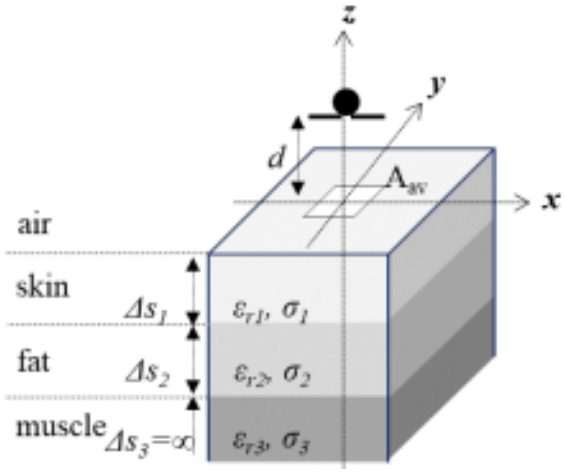

Relative electric permittivity and electric conductivity for skin, fat and muscle at 10, 30 and 90 GHz

Layers	**f**=10 GHz		**f**=30 GHz		**f**=90 GHz	
	σ (S/m)	ε_r	**σ (S/m)**	ε_r	**σ (S/m)**	ε_r
Skin	8.4824	32.409	27.31	16.63	41.94	6.826
Fat	0.585	4.602	1.794	3.639	3.411	2.931
Muscle	10.63	42.76	35.49	23.16	60.72	9.304

Δs_1=1.5 mm

Δs_2=4 mm,

Δs_3=∞

d=5, 10, 15 mm for 10 and 30 GHz

d=2, 5, 10 mm for 90 GHz

CONCLUDING REMARKS

ICEAA INTERNATIONAL CONFERENCE ON ELECTROMAGNETICS IN ADVANCED APPLICATIONS
IEEE APWC IEEE-APS TOPICAL CONFERENCE ON ANTENNAS AND PROPAGATION IN WIRELESS COMMUNICATIONS
SEPTEMBER 8-12, 2025
PALERMO, ITALY

- The paper deals with the influence of 3different voltage source models;

  - Delta gap (DG)
  - Magnetic frill (MF)
  - Magntetic current loop (MCL)

to current distribution, radiated field and input admittance of dipole antenna in free space and above a lossy half-space when used in GHz frequency range.

- Some illustrative numerical results are presented.
- The future work will deal with an influence of different source models to the behaviour of dipole antenna above multilayered half-space.

Thank you for your attention!

Prof. Dragan Poljak, PhD

University of Split,

Faculty of Electrical Engineering, Mechanical Engineering and Naval Architecture